Received: 11 November 2021 | Revised: 7 December 2021 | Accepted: 7 December 2021

DOI: 10.1002/bkcs.12453

REVIEW

BKCS BULLETIN OF THE KOREAN CHEMICAL SOCIETY

Tunneling dynamics dictated by the multidimensional conical intersection seam in the πσ*-mediated photochemistry of heteroaromatic molecules

Junggil Kim[1] | **Kyung Chul Woo**[1,2] | **Kuk Ki Kim**[1] | **Minseok Kang**[1] | **Sang Kyu Kim**[1]

[1]Department of Chemistry, KAIST, Daejeon, Republic of Korea

[2]Division of Chemistry and Biological Chemistry, School of Physical and Mathematical Sciences, Nanyang Technological University, Singapore, Singapore

Correspondence
Sang Kyu Kim, Department of Chemistry, KAIST, Daejeon 34141, Republic of Korea.
Email: sangkyukim@kaist.ac.kr

Funding information
National Research Foundation of Korea, Grant/Award Numbers: 2019R1A6A1A10073887, 2019K1A3A1A14064258, 2018R1A2B3004534

Abstract

The πσ*-mediated photochemistry of heteroaromatic molecules has provoked the investigation of the conical intersection dynamics. The Born–Oppenheimer approximation fails at the conical intersection where the S_1 (ππ*) and S_2 (πσ*) states cross. The nonadiabatic transitions are much influenced by the nuclear configuration of the reactive flux particularly in the curve-crossing region encountered along the reaction pathway. In this article, we focus on the tunneling dynamics of phenols and thiophenols. The O (S)—H bond cleavage occurs via tunneling through the barrier which is dynamically shaped by the upper-lying S_1/S_2 conical intersection in terms of the couplings at the individual branching planes as well as along the (3N-8) dimensional seam coordinates. State-specific tunneling rates and their interpretation are given for phenol, substituted phenols, thiophenol, *ortho*-substituted thiophenols, and benzenediols including their 1:1 water clusters. The completely orthogonal modes to the tunneling coordinate are very critical in the dynamic shaping of the reaction barrier.

KEYWORDS
Born–Oppenheimer approximation, excited state, heteroaromatic molecules, photodissociation, tunneling

INTRODUCTION

The πσ*-mediated photochemistry in heteroaromatic molecules has been both extensively and intensively studied for many recent decades.[1–8] The efficient coupling of the optically bright S_1 (ππ*) state with the upper-lying optically darker S_2 (πσ*) state gives rise to the conical intersection where the nonadiabatic transition is supposed to be much facilitated.[9–12] The Born–Oppenheimer approximation fails in the vicinity of the conical intersection, and one should deal with the situation where the nuclear motion does not stick to the adiabatic potential energy surface anymore.[13–18] As surface crossings are ubiquitous in the excited states, many photochemical and photobiological processes undergo nonadiabatic transitions through conical intersections encountered along their reaction pathways. The πσ*-mediated photochemistry, in this aspect, is quite unique as it gives the rational explanation for the ultrafast nonradiative transitions of many heteroaromatic molecular systems upon the electronic excitations, which are often relevant to the photochemical or photobiological activities.[6,19–38] As a matter of fact, spectroscopic and dynamic studies on heteroaromatic systems including phenols,[9,12,39–75] thiophenols,[10–12,76–97] anisoles,[98–102] thioanisoles,[5,103–115] or many others are vast in terms of their diversities and detailed dynamic features. Herein, we focus on the H-atom detachment reactions of phenols and thiophenols especially in terms of the state-specific tunneling rate constants.

The O—H (or S—H) bond dissociations of phenols (or thiophenols) in the S_1 state take place via tunneling through the reaction barrier which is the consequence from the curve-crossing of the bound S_1 (ππ*) and unbound S_2 (πσ*) state. The tunneling reaction is then

Junggil Kim and Kyung Chul Woo contributed equally to this study.

governed by the S_1/S_2 conical intersection in terms of its multidimensional structure and dynamic role especially in nonadiabatic transitions. As the S_2 state is repulsive along the O—H (or S—H) bond extension coordinate, the tunneling from the bound S_1 to the unbound S_2 leads to the H-atom detachment reaction. In the planar geometry where the O—H (or S—H) bond axis lies on the plane of the benzene moiety, the wave packet sliding on the repulsive S_2 state experiences another conical intersection located in the later stage of the reaction pathway. This second conical intersection results from the curve crossing of S_2 (which is diabatically correlated to the ground (thio-)phenoxyl radical ($\tilde{X}$)) with the S_0 state (diabatically correlating to the electronically excited (thio-)phenoxyl radical ($\tilde{A}$)) at the asymptotic limit (Figure 1).[4,12,59,76] Nonadiabatic transition at the second S_0/S_2 conical intersection gives rise to the ground state of the (thio-)phenoxyl radical whereas the excited state of the (thio-)phenoxyl radical is generated by the adiabatic pathway. The nonadiabatic transition probability at the S_0/S_2 conical intersection could be then precisely estimated experimentally by measuring the branching ratio of these pathways from translational energy distribution of the H-fragment,[10–12,76–78,83] providing the great opportunity to understand and control the conical-intersection dynamics in the state and structure specific ways.[11,77,80–83,86,93–95] The rate of the whole reaction though is governed by that of the tunneling process through the barrier which is dynamically shaped by the S_1/S_2 conical intersection.[54,96,116–121] It should be emphasized that the tunneling dynamics of phenols (or thiophenols) is multidimensional in nature although the tunneling process could be regarded to occur along the one-dimensional O—H (or S—H) bond extension coordinate. This is because that the tunneling barrier is dynamically shaped along the branching plane as well as (3*N*-8) dimensional seam coordinates of the conical intersection.[58,61,64,88–90,122] Multidimensional aspects of the tunneling could be clearly manifested in the mode-dependent tunneling rates measured for phenols and thiophenols.[69,73,85,96,117,121]

In this mini-review, we try to summarize and give the perspective mainly based on a series of recent works from our own group although it should be emphasized that this review would not be possible without the contribution of a number of beautiful works from other prominent research groups. Thus, it should be noted that this article may not provide the complete survey of literatures on the tunneling dynamics of phenols or thiophenols. In the main text, the characters of the excited states of the heteroaromatic systems will be briefly explained. The overall features of the potential energy surfaces along the tunneling coordinate are quite similar for both phenols and thiophenols. State-specific tunneling rate measurements and their interpretations will be then given for (i) phenol, (ii) substituted phenols such as *o*-cresol (2-methylphenol), (iii) thiophenol, (iv) *ortho*-substituted thiophenols (2-methoxythiophenol, 2-fluorothiophenol, and 2-chlorothiophenol), and (v) benzenediols (catechol, resorcinol, and hydroquinone) and their 1:1 water clusters. Finally, the perspective on the subject is briefly given.

THE TUNNELING DISSOCIATION OF THE O—H BOND IN THE S_1 STATE OF PHENOLS

Phenol: The prototypical system of the πσ*-mediated photochemistry

Phenol is one of the most studied systems in the field of photochemistry not only because it is the simplest heteroaromatic system but also because its photochemistry is quite relevant to the biological activities in certain circumstances.[6,36] Though the photochemistry of phenol had long been investigated, the important role of the S_2 (πσ*) state in the nonadiabatic transitions of the excited states was realized not so long ago.[1,2,39] For instance, the Ni group has identified the fast H-atom fragmentation from phenol excited at 193 and 248 nm using their multimass ion imaging apparatus[40,43] whereas the Ashfold group has analyzed the detailed coupling mechanism of the O—H dissociation reaction by means of the highly resolved Rydberg-tagging H-atom translational spectroscopy.[41,48,50] It is now well established that the optically bright bound S_1 (ππ*) state is strongly coupled to the upper-lying unbound S_2 (πσ*) state to give rise to the fast H-atom fragment, as depicted in Figure 1. The S_1 state lifetime of phenol had been numerously estimated from various spectroscopic and time-resolved studies at the zero-point vibrational energy level,[116,123–127] giving

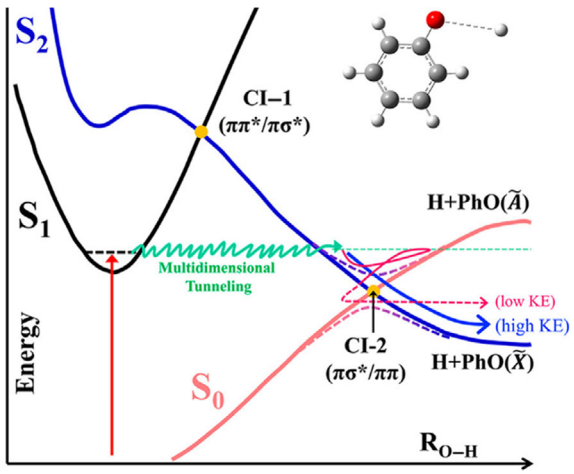

FIGURE 1 Schematic potential energy curves along the O—H tunneling coordinate in phenol. The reactive flux tunneled through the barrier under the S_1/S_2 conical intersection slides on the repulsive S_2 state to give high or low kinetic energy H-atom fragments revealing the nonadiabatic transition at the S_0/S_2 conical intersection (see the text). Adapted from Ref. 73 using the potential energy surfaces calculated by Ref. 59

$\tau \sim 2.5$ ns for the S_1 origin, for instance, from the femtosecond (fs) time-resolved pump-probe method by the Stavros group.[53] The S_1 lifetime reflects the sum of rates of all possible S_1 decay pathways, and the radiative and nonradiative transition rates (the S_0–S_1 internal conversion and/or T_1–S_1 intersystem crossing) contribute to the decay of the S_1 phenol at its zero-point level quite significantly.[41,123–128] Actually, the quantum yield of the H-atom tunneling at the S_1 origin had been estimated to be ~0.83, indicating that the tunneling rate is about five times faster than the sum of other decay rates at the S_1 zero-point level.[124] This in turn though suggests that the measured S_1 lifetime of phenol is mostly determined by the H-atom tunneling rate. Because of the intrinsic broad bandwidth of the fs laser pulse, the state-specific tunneling rate of the S_1 phenol could not be invoked until quite recently.[69,73] The Tseng group firstly used the picosecond (ps) pump-probe method to obtain the parent ion transients at several different S_1 vibronic modes of phenol, showing the dramatic mode-dependency of the tunneling rates.[69] The more complete ps-resolved tunneling rates for the properly assigned S_1 vibronic bands as well as the associated H-atom translational distributions have been precisely measured by our own group,[73] revealing the multidimensional nature of the tunneling reaction and nailing down the otherwise controversial origins of the slow and fast H-atom fragment.[41,50,53,129] The fast H-atom fragment with the Gaussian-shaped translational distribution results from the funneling into the S_0/S_2 conical intersection, whereas the slower H-fragment should represent the reactive flux which undergoes the vibrational predissociation process along the adiabatic potential surface generated under the S_0/S_2 conical intersection.[58,130]

Consistently with the previous studies,[53,69,116,123–127] the lifetime (τ) at the S_1 origin is found to be ~2.3 ns. Thereafter, however, the S_1 lifetime gets largely fluctuated with the dramatic mode-dependency especially in the low excitation energy region of 0–1200 cm^{-1}, where the intramolecular vibrational redistribution (IVR) is not turned on yet due to the low density of states (Figure 2). For instance, the lifetime gets slightly decreased to ~1.9 ns at 324 cm^{-1} (11^2) whereas it increases to ~2.9 ns at 374 cm^{-1} ($16a^2$). Interestingly, the $16a^2$ mode was reported to be highly activated in the product-state distributions.[41,44,50] The experimental finding that the tunneling rate at the $16a^2$ mode excitation is slowed down thus seems to be contradictory at the first impression. On the other hand, it may suggest that the $16a^2$ mode is indeed coupled to the tunneling coordinate but in a way of impeding the tunneling rate. The reactive flux inside the S_1 well is then somehow retained along the 16a normal mode to be manifested in the final product energy release. The S_1 lifetime gets converged to $\tau \sim 800$ ps at the S_1 internal energy of 3600 cm^{-1} where the given internal energy is expected to be randomized among isoenergetic states. Actually, the tunneling rate starts to be converged without the mode-dependency at the S_1 internal energy of ~1200 cm^{-1}, suggesting that the IVR rate from thereon is now comparable to or faster than the tunneling rate. It is quite notable that the slow IVR rate in the low internal energy of S_1 gives the great opportunity to disentangle the govern the dynamic shaping of the associated multidimensional tunneling barriers. Tunneling rates of phenol clearly demonstrate that the tunneling cannot be explained by the one-dimensional picture

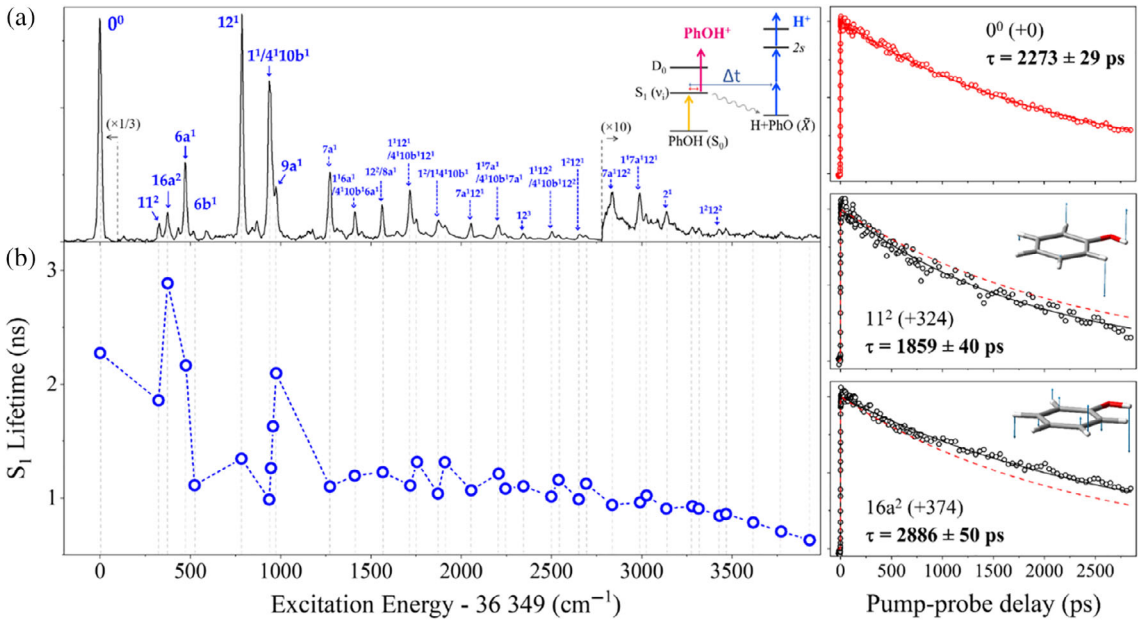

FIGURE 2 (a) Picosecond (1 + 1′) resonance-enhanced two-photon ionization (R2PI) spectrum of the S_1 state phenol. (b) Mode-specific tunneling rates of phenol obtained from the time-resolved pump-probe parent ion yield transients. Some transients at the S_1 zero-point energy level (red), 11^2 mode, and $16a^2$ modes (black) are shown on the right panel with the single exponential fits

alone. The strong mode-dependent tunneling rates confirm that the tunneling dynamics is strongly influenced by the multidimensional nuclear configurations spanned by the specific vibronic mode excitations. As the tunneling barrier is shaped by the S_1/S_2 conical intersection, its shape with respect to the multidimensional coordinates is dictated by the magnitudes of the nonadiabatic coupling matrix elements which are strongly dependent on the individual coupling mode characteristics.[62–64,131,132]

The one-dimensional barrier height for the O—H tunneling of the S_1 phenol at the fixed planar geometry had been predicted to be 7000–8500 cm^{-1}.[9,50,53,58,62] From the simplistic assumption, one may calculate the one-dimensional tunneling rate by the semi-classical theory using the Wentzel–Kramers–Brillouin (WKB) approximation, which is sensible and yet overestimating the experiment.[53,116,120,121] As a matter of fact, tunneling dynamics of phenol has been subject to many high-level dynamic calculations for recent years.[9,42,44,51,59,62–67,70,71,74,75] For instance, Guo and colleagues reported that the O—H tunneling rate of phenol calculated on the full-dimensional potential energy surfaces does not reproduce the experiment without the consideration of the geometric phase which is inevitable in the nonadiabatic transition where the reactive fluxes encircles the conical intersection.[62–64,74] The geometric phase issue in the tunneling process is extremely interesting, and the experimental demonstrations would be highly desirable in the near future as the excited-state dynamics of phenol (or thiophenol) is one of the ideal targets for resolving this important problem.

It is quite notable that the prominent quantum beats have been observed for several Fermi-doublets in the S_1 phenol.[133] For example, the Fermi-doublet located at the S_1 internal energy of 935 and 938 cm^{-1} (Figure 2) represent a couple of eigenstates resulting from the Fermi-type coupling of the optically bright 1^1 fundamental and optically dark $4^1 10b^1$ combinational modes (Figure 3).[134,135] Within the coherent width of the picosecond pump laser pulse ($\Delta t \sim 1.5$ ps), this doublet is coherently excited to give the largely modulated quantum beat in the ionization cross section. The Fourier transform of the interferogram then gives the gap of 3.302 ± 0.001 cm^{-1} between the Fermi doublet with the great precision. The largely modulated quantum beat survives during the entire S_1 lifetime of 2.9 ns, confirming that the dissipative IVR does not take place within the tunneling lifetime even at the internal energy of ~1000 cm^{-1}.[73] Moreover, the sharply contrasted quantum beat seems to open the great opportunity to investigate the nonstationary quantum state as the superposition of Fermi-doublet could be almost completely decomposed into the zeroth-order states in the temporal domain. One may then select the otherwise mixed zeroth-order state by choosing the particular delay time between pump and probe laser pulses. It still sounds quite challenging, and yet this temporal isolation could be conceptually employed for the investigation for the mode effect of the spectroscopically inseparable mixed-eigenstates.

Substituted phenols: The role of the conical intersection (multidimensional) seam coordinate

Chemical derivatives of phenol including fluorophenol, chlorophenol, bromophenol, iodophenol, or methylphenol (cresol) have been much studied to date.[100,116–121,136–151] Depending on the *ortho*(*o*), *meta*(*m*) or *para*(*p*) position of the substituent on the phenol ring with respect to the OH moiety, the associated dynamics is apparently quite different. In general, the substitution on the *meta*- or *para*-position of phenol does not seem to be much influential on the O—H bond cleavage dynamic in terms of the tunneling rate and the excess energy disposal dynamics,[116,120,138,142,143,145–151] except the presence of the additional chemical bond

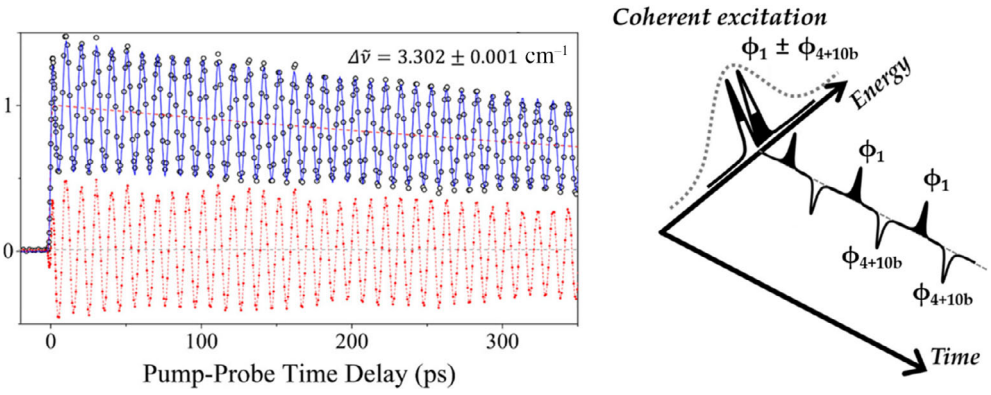

FIGURE 3 (Left) Quantum beats of the parent ion signal in the picosecond time-resolved pump-probe measurement after the photoexcitation of the $1^1/4^1 10b^1$ Fermi doublet of the S_1 state phenol. The upper panel with open dots is experimental data points and the lower panel with filled symbols represents the residuals after subtracting the exponentially decaying component. (Right) Schematic showing the complete decomposition of the Fermi doublet into the zeroth-order states in the temporal domain

cleavage channels introduced especially for the bromo- or iodo-phenol, for example.[137,141] The *ortho*-substitution, on the other hand, gives rise to the substantial changes in the whole reaction dynamics. As a prototypical case, the most dramatic change has been observed in the S_1 dynamics of 2-chlorophenol.[147,152] Namely, the S_1 lifetime is found to be ultrashort which is less than a picosecond for the *syn*-conformer of 2-chlorophenol,[147] suggesting that the O—H tunneling is not the major channel anymore for the S_1 state of *syn*-2-chlorophenol. The strong intramolecular O—H···Cl hydrogen bonding seems to be responsible for the ultrafast nonradiative decay presumably through the S_1/S_0 conical intersection extended along the C—Cl bond extension coordinate. The S_1 relaxation dynamics of 2-chlorophenol, by itself, is extremely interesting. The associated reaction mechanism in terms of the various product channels, nonradiative transition rates, or the dynamic role of the intramolecular hydrogen-bonding is still subject to the further detailed investigation.

Another very interesting system turns out to be the 2-methylphenol (*o*-cresol) molecule.[116,121] *o*-Cresol adopts either *cis* or *trans* conformational isomer, and both are significantly populated in the molecular jet. Quite interestingly, the S_1 lifetime of *cis*-*o*-cresol at its origin is found to be ~1.8 ns (from the biexponential fit, vide infra), which is quite similar to that of phenol.[121] This suggests that the O—H tunneling dynamics and the competitive nonradiative transition rates are little influenced by the CH_3 substitution on the *ortho*-position in the *cis*-conformational structure. Remarkably, however, the S_1 decay dynamics of *trans*-*o*-cresol has been found to be dramatically different from that of phenol in many ways. First of all, the S_1 lifetime at the origin is estimated to be ~700 ps (Figure 4), indicating that the tunneling barrier of the *trans* conformer should be significantly lower than that of the *cis* conformer.[116,121] More interestingly, the O—H tunneling rate of *trans*-*o*-cresol is found to be strongly dependent on the eigenstates associated with the CH_3 internal rotation with respect to the phenol moiety. In the very narrow energetic region (0–150 cm^{-1}), the tunneling lifetime varies in the wide dynamic range ($\tau \sim$ 697–419 ps). The *trans*-*o*-cresol undergoes the structural change upon the S_1–S_0 excitation with respect to the methyl internal rotor, giving a number of highly excited CH_3 internal rotor states as manifested in the resonance-enhanced two-photon ionization (R2PI) spectrum (Figure 4). The tunneling rate ($\tau \sim$ 697 ps) at the zero-point level ($0a_1/1e$) increases with the CH_3 rotor-level excitation ($\tau \sim$ 493 or ~ 419 ps for the 2e or $3a_1$ state, respectively), and yet it falls back again with increasing

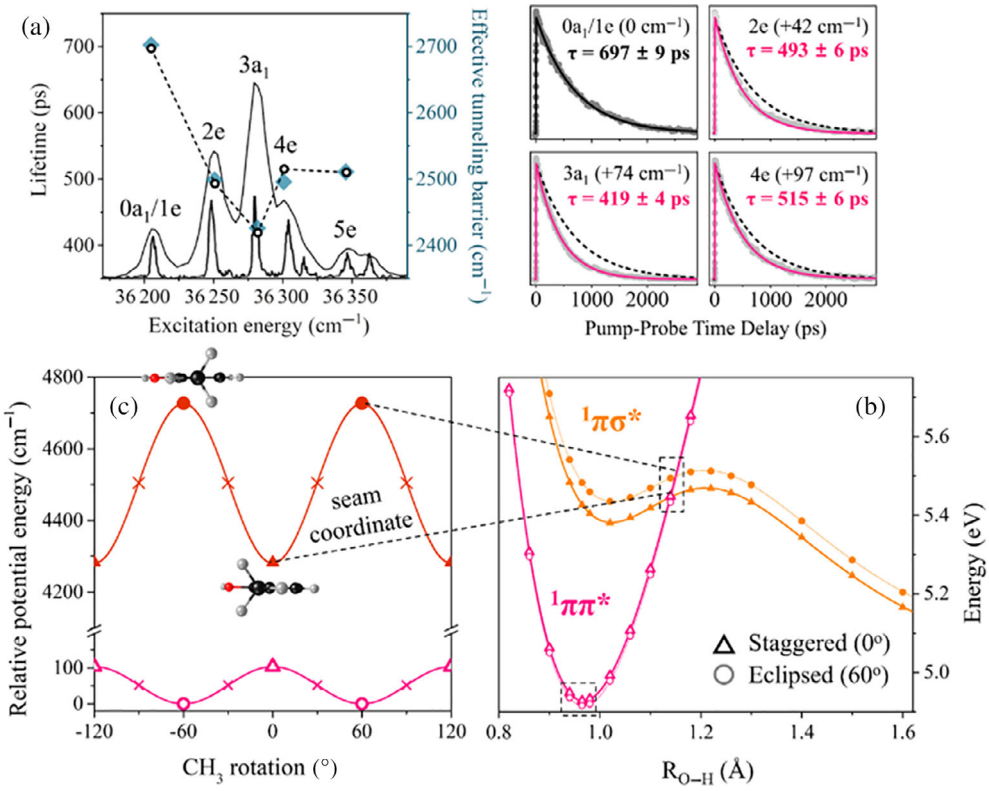

FIGURE 4 The O—H tunneling rate dictated by the CH_3 torsional mode excitation. (a) The tunneling lifetimes of S_1 *trans*-*o*-cresol at different CH_3 torsional levels. The effective tunneling barrier calculated for each CH_3 torsional state is overlaid with the experimental lifetime. (b) Potential energy curves of S_1 ($^1\pi\pi^*$) and S_2 ($^1\pi\sigma^*$) states along the O—H bond extension coordinate for the staggered (triangle) or eclipsed (circle) CH_3 geometry with respect to the OH moiety. (c) The CH_3 torsional potential energy curves represented by the sinusoidal functions at the S_1/S_2 crossing point (orange) and the S_1 minimum (pink)

the internal energy ($\tau \sim 515$ or ~ 510 ps at 4e and 5e, respectively).

As the CH_3 moiety is geometrically remote in the *trans* conformer and its internal rotation seems to be irrelevant to the OH tunneling coordinate from the perspective of the S_1/S_2 conical intersection where the most influential coupling coordinate should be the C_2—C_1—O—H dihedral torsional angle, it could sound quite counterintuitive that the O—H tunneling rate is modulated by the CH_3 internal rotor quantum states. In the ground electronic state (S_0) of the *trans-o*-cresol, the CH_3 moiety with respect to the molecular plane adopts the staggered geometry. As the CH_3 torsional barrier height in S_0 is $\sim$355 cm^{-1}, only the nearly degenerate $0a_1/1e$ states of the zero-point level are populated in the molecular jet. Upon the S_1–S_0 transition, the *trans-o*-cresol undergoes the structural change from the staggered to eclipsed geometry, where the S_1 torsional barrier height is precisely estimated to be 83 cm^{-1}.[153–155] According to the equation of motion coupled cluster singles and doubles (EOM-CCSD) calculations of S_1 and S_2 surfaces, the CH_3 torsional barrier in the S_1 state is calculated to be $\sim$0.01 eV for both conformers, which is in excellent agreement with the previous report.[153] Quite amazingly, on the other hand, the CH_3 staggered geometry is calculated to be more stable than the eclipsed geometry in the S_2 ($^1\pi\sigma^*$) state of the *trans* conformer. The torsional potential at the conical intersection is the sinusoidal function with the eclipsed and staggered conformations as crest and trough, respectively, with the calculated conformational barrier of $\sim$400 cm^{-1} (Figure 4). This indicates that the S_1/S_2 conical intersection is extended into the seam coordinate of the CH_3 torsional angle, suggesting that the CH_3 internal rotation may play an essential dynamic role as one of the (3*N*-8) dimensional seam coordinates. This gives the extremely interesting dynamic feature regarding the relationship between the molecular geometry and tunneling dynamics. Namely, the tunneling barrier for the S_1 reactive flux is determined by the energetics and nuclear configuration of the S_1/S_2 conical intersection with the eclipsed (crest) or staggered (trough) geometry developed along the CH_3 torsional seam coordinate, respectively, indicating that the O—H tunneling barrier should be much higher for the eclipsed geometry compared to that for the staggered geometry. The tunneling barrier for the eclipsed and/or staggered geometry is weight averaged according to the square of the wave function of each CH_3 torsional quantum level over the nuclear configuration of the entire 0–2π torsional angle, giving the estimation for the "effective" tunneling barrier for each CH_3 internal rotor level, giving the perfectly matched effective torsional barrier with the experiment (Figure 4). This example, for the first time, demonstrates experimentally that the extension of the conical intersection into the seam coordinate is quite essential in dictating the multidimensional tunneling reactions. Notably, dynamics of the *cis-o*-cresol conformer needs the further investigation.

As shown in Figure 4, the S_1 parent transient (at the origin) shows the biexponential behavior, giving the faster component with $\tau \sim 1.8$ ns whereas the lifetime of the slower component could be more than 10 ns. In the rather narrow 0–3.0 ns temporal window, however, extracting the exact time constants is not totally reliable. The observation of the biexponential behavior in the transient is quite rare in the simple kinetic scheme as the distinct reactive fluxes should have been prepared in the initial photo-excitation as the parent transient otherwise would show the single-exponential behavior regardless of the number of different reaction pathways.

THE TUNNELING DISSOCIATION OF THE S—H BOND IN THE S_1 STATES OF THIOPHENOLS

Thiophenol: The ultrafast S—H bond rupture gives the high nonadiabatic transition probability

The S_1-state dynamics of thiophenol is quite similar to that of phenol in terms of overall features regarding conical intersections of S_0, S_1 ($\pi\pi^*$), and S_2 ($\pi\sigma^*$) along the S—H bond extension coordinate, as depicted in Figure 5. And yet, its detailed dynamics is very different especially in terms of energetics. One of the most distinct differences could be found in the energetics of the final products of the ground and first excited state of the thiophenoxyl radical ($C_6H_5S\cdot$). The difference between the ground ($\widetilde{X}$) and the first electronically excited ($\widetilde{A}$) states of the $C_6H_5S\cdot$ radical has been precisely measured to be $\sim$3000 cm^{-1}.[156] This is much smaller than the gap of $\sim$7700 cm^{-1} between $\widetilde{X}$ and $\widetilde{A}$ states of the $C_6H_5O\cdot$ radical for phenol.[157] Therefore, differently from the case of phenol, both the $\widetilde{X}$ and $\widetilde{A}$ states of the $C_6H_5S\cdot$ radical are produced even at the S_1 origin level of thiophenol. This indicates that the nonadiabatic transition probability could be quantitatively estimated for thiophenol as the $\widetilde{X}$ state of $C_6H_5S\cdot$ originates from the nonadiabatic funneling into the S_0/S_2 conical intersection while the adiabatic path avoids the S_0/S_2 conical intersection to generate the $\widetilde{A}$ state of the C_6H_5S radical at the asymptotic limit. The H or D fragment translational distributions from thiophenol (C_6H_5SH) or thiophenol-d_1 (C_6H_5SD), respectively, have been obtained by the velocity-map ion imaging method.[10,11,76,77,83] The relative ratio of the high- to the low-kinetic energy portions gives the $\widetilde{X}/\widetilde{A}$ product branching ratio which increases with the increase of the nonadiabatic transition probability. The $\widetilde{X}/\widetilde{A}$ product branching ratio at the S_1 origin of thiophenol-d_1 is estimated to be $\sim 0.75 \pm 0.15$ and remains more or less constant over the 0–2000 cm^{-1} range.[83] This indicates that the quite large portion of the reactive flux funnels through the conical intersection, disobeying the Born–Oppenheimer approximation. On the two-dimensional branching plane of the conical intersection (for both S_1/S_2

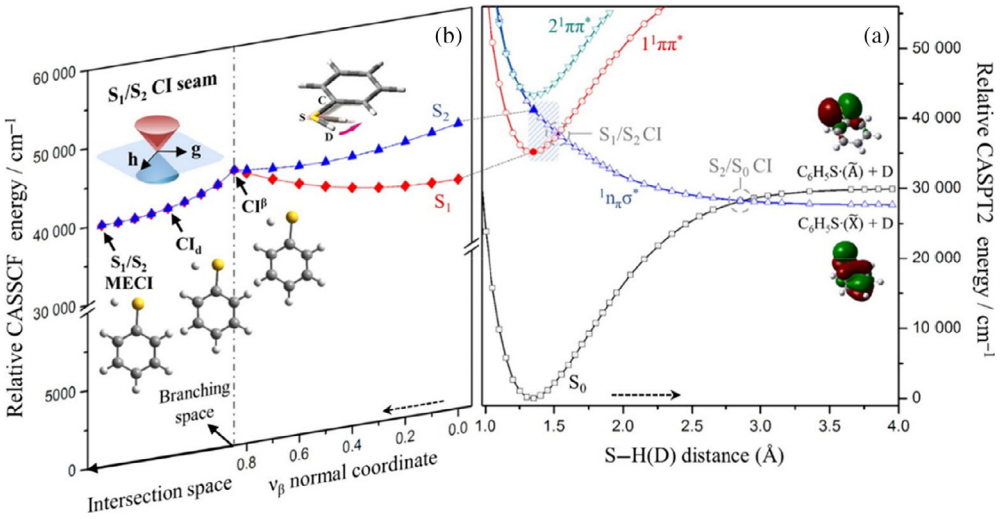

FIGURE 5 (a) Potential energy curves of the S_0, $1^1\pi\pi^*$, $^1\pi\sigma^*$, and $2^1\pi\pi^*$ states of thiophenol along the S—H(D) bond extension coordinate at the planar geometry, calculated using CASPT2//SA4-CASSCF(12,11) level of theory. (b) Potential energy profiles of the S_1 and S_2 states of thiophenol along the CSH(D) bending vibrational mode (β) coordinate where the β-mode conical intersection (CI^{β}) is connected to the minimum energy conical intersection (MECI) along the seam coordinate (adapted from Ref. 83)

and S_0/S_2), the gradient vector is along the S—H (D) extension coordinate whereas the most influential coupling vector is parallel to the C_2—C_1—S—H(D) dihedral torsional angle (ϕ).[81–83,87–90] In other words, when $\phi \approx 0°$ (planar), the probability of the reactive flux to funnel through the conical intersection is expected to be high whereas it should be significantly reduced as the molecule becomes nonplanar with the increase of the torsional angle ($\phi \neq 0°$). Utilizing this fact, the nonadiabatic transition probability could be largely controlled by the manipulation of the conformational structure of thiophenol by the chemical substitution.[11,80,86,93–96] Namely, for instance, the $\widetilde{X}/\widetilde{A}$ product branching ratio of ~0.75 at the 243 nm excitation estimated for thiophenol-d_1 is much reduced to ~0.10 for *para*-methoxythiophenol-d_1.[11] This is mainly attributed to the perpendicular orientation of the S—D bond axis with respect to the molecular plane of *para*-methoxythiophenol-d_1 in S_0, compared to the planar geometry of thiophenol.[80,158] Upon the vertical excitation at 243 nm, the ultrafast S—D bond rupture of *para*-methoxythiophenol-d_1 takes place on the nonplanar geometry to avoid the S_0/S_2 conical intersection to follow the adiabatic reaction path rather exclusively.

The S_1 lifetime of thiophenol (or thiophenol-d_1) has been estimated to be 50–60 (or 70–80) fs from the spectroscopic features[78,83] or real-time transients.[85,159] This indicates that the S—H(D) bond rupture occurs promptly with a very small tunneling barrier, although the tunneling barrier should not be taken to be one-dimensional. In this regard, the one-dimensional potential energy surface as depicted in Figure 5 hardly explains the experiment (the multidimensionality of the tunneling dynamics will be more discussed in Section 3.2). Anyhow, the ultrafast S—H(D) bond rupture is quite consistent with the high probability of the nonadiabatic transition of thiophenol, giving the large $\widetilde{X}/\widetilde{A}$ product branching ratio of ~0.75 at the asymptotic limit (vide supra). The reactive flux prepared on S_1/S_2 proceeds very fast, and thus the molecular planarity maintains at the S_0/S_2 conical intersection to give the high nonadiabatic transition probability. More interestingly, it has been found that the product angular distribution is sharply varied with increasing the S_1 internal energy of thiophenol.[83] As the S—H(D) bond breakage occurs much faster than the rotational period, the anisotropy parameter (β) from $I(\theta) = (\sigma/4\pi) \cdot [1 + \beta \cdot P_2(\cos\theta)]$ is expected to be positive for the angular distribution of D from the S_1 thiophenol-d_1 as the transition dipole moment of the S_1–S_0 transition is parallel to the S—H (D) bond axis. Here θ is the angle between the direction of the fragment velocity and the electric vector of linearly polarized light, σ is the absorption cross section, and P_2 is the second-order Legendre polynomial. As a matter of fact, β is estimated to be +0.25 at the S_1 origin. And yet, β is found to decrease sharply with increasing of the S_1 internal energy to give the negative value of −0.60 before going back to nearly zero again, giving a broad peak ($\Delta E \approx 200\,cm^{-1}$) in β centered at the S_1 internal energy of ~600 cm^{-1}. This peculiar β-dip could be explainable by invoking the S_2–S_0 transition dipole moment of which the direction is perpendicular to both the benzene plane and the S—D bond axis.[77] The β-dip observed at 600 cm^{-1} above the S_1 origin of thiophenol-d_1 should be then due to the excitation of a particular vibronic band through which the nuclear configuration near the S_1/S_2 conical intersection seam is accessed (Figure 5). As the explored phase space volume accessed by the one-photon excitation is limited by the Franck–Condon window, the multidimensional aspects of the S_1/S_2 conical intersection still

need the further refinement by other means in the near future.

The thiophenol system seems to be quite ideal for studying the nonadiabatic dynamics as one can quantitatively measure the nonadiabatic transition probability.[87–90] Namely, one can tune the various quantum variables such as the electronic (or internal) energy or vibronic quantum numbers to interrogate the relationship between the quantum state and nonadiabatic dynamic behavior, giving the rare opportunity to unravel the structure and dynamic role of the conical intersection in a state-specific way. The geometric phase which has been theoretically invoked in the situation where the reactive flux encircles the conical intersection (vide supra) should also be applied to the case of the prompt S—H bond dissociation of thiophenol. Compared to the case of phenol, the S_1/S_2 conical intersection is located quite close to the S_1 origin for thiophenol (Figures 1 and 5), ensuring the ultrafast nuclear motion in the proximity of the conical intersection. Therefore, one can think of the preparation and real-time monitoring of the S_1 coherent wave packet which undergoes the constructive or destructive interference by the encircling reactive fluxes due to the geometric phase. For this experiment, one many need the ultrashort (<<10 fs) laser pulse as well as the new experimental scheme to overcome the Franck–Condon limit in the optical excitation, which is challenging but will be quite rewarding in terms of figuring out the role of the geometric phase in real-time.

Substituted thiophenols: Dynamic shaping of the tunneling barrier by the upper-lying conical intersection

The S—H(D) bond dissociation of the S_1 (or S_2) thiophenol is ultrafast (<<100 fs), as described in Section 3.1, and thus the investigation of the vibronic mode dependence of the tunneling rate is intrinsically nontrivial as the lifetimes of all accessible S_1 modes of thiophenol are much shorter than 100 fs which is beyond the experimental limit. In order to study the slowed-down tunneling process, dynamics of three *ortho*-substituted thiophenols have recently been investigated.[93–97] These include 2-methoxythiophenol (2-MTP; 2-CH_3O-C_6H_4SH), 2-fluorothiophenol (2-FTP; 2-F-C_6H_4SH), and 2-chlorothiophenol (2-CTP; 2-Cl-C_6H_4SH). Remarkably, the S—H(D) bond dissociation is significantly slowed down in all three substituted thiophenols, giving the great opportunity to interrogate the vibronic mode dependency of the tunneling rate in quite details. For instance, the R2PI spectra using the nanosecond laser pulse provide the well-resolved S_1 vibronic structures of 2-MTP,[95] 2-FTP, and 2-CTP,[93] indicating already that the corresponding S_1 lifetimes are much longer than those of thiophenol. In *ortho*-substituted thiophenols, due to the presence of the rather strong intramolecular hydrogen bonding (S—H···O, S—H···F, or S—H···Cl for 2-MTP, 2-FTP, or 2-CTP, respectively), the overall nonadiabatic transition probabilities (equivalent to the $\widetilde{X}/\widetilde{A}$ product branching ratios) are found to be quite higher than those of thiophenol in the S_1 state.[93,95] For 2-MTP, it has been estimated to be more than 2.0 (compared to 0.75 for thiophenol) near the S_1 origin, strongly indicating that the intramolecular hydrogen-bonding tends to maintain the molecular planarity throughout the reaction pathway. Particularly, in the low S_1 internal energy less than $\sim$500 cm^{-1}, the $\widetilde{X}/\widetilde{A}$ product branching ratio remains above $\sim$1.0 for all of 2-MTP, 2-FTP, and 2-CTP, suggesting that the intramolecular hydrogen bonding plays an important role in the enhancement of the nonadiabatic transition probability for all three molecules. As the S_1 internal energy increases, however, the nonadiabatic transition probability at the S_0/S_2 conical intersection dramatically decreases for 2-MTP and 2-FTP. This may suggest that the reactive flux becomes more flexible along the out-of-plane coordinate as the internal energy increases above the SH out-of-plane torsional barrier for 2-MTP and 2-FTP. When the IVR rate is comparable to or faster than the tunneling rate, the $\widetilde{X}/\widetilde{A}$ product branching ratio seems to be unchanged with increasing the internal energy. For thiophenol, the $\widetilde{X}/\widetilde{A}$ product branching ratio is independent of the S_1 internal energy (vide supra)[83]; this is most likely due to the ultrafast (<<100 fs) S—H(D) bond rupture in the wide energetic range of the S_1 internal energy. Namely, the ultrafast S—H(D) dissociation pathway more or less remains same in nature regardless of the excitation of the vibrational modes which are orthogonal to the S—H(D) extension coordinate. Notably, the $\widetilde{X}/\widetilde{A}$ product branching ratio is also not influenced by the S_1 internal energy for 2-CTP.[93] Actually, the dynamics of 2-CTP is quite unique in terms of its diversity of the S_1 decay pathways. In 2-CTP, although the S—H bond rupture takes place by tunneling, its quantum yield seems to drastically decrease with increasing the S_1 internal energy,[96] indicating that the new decay channel may be opened at the relatively low internal energy. Further investigation of different decay channels of the 2-CTP (S_1) is quite desirable in the near future.

The H-atom detachment rate has been measured by the picosecond pump-probe scheme for 2-MTP, 2-FTP, and 2-CTP.[96] Individual vibronic modes could be well resolved and their mode characters could be well isolated by employing the slow-electron velocity-map imaging spectroscopy and ab initio calculations. Indeed, compared to the case of thiophenol, the tunneling rate of 2-MTP, 2-FTP, or 2-CTP is found to be significantly slowed down. Namely, the picosecond time-resolved parent ion transient at the S_1 origin of 2-MTP shows a single exponential decay with a lifetime of $\sim$44 ps (Figure 6). The rate measurement of the monodeuterated sample, 2-methoxythiophenol-d_1 (2-MTP-d_1), gives the huge primary kinetic isotope effect on the tunneling rate, giving $\tau \approx 640$ or 410 ps at the S_1 origin or τ_{MeO2} (101 cm^{-1}) band excitation of 2-MTP-d_1, respectively,

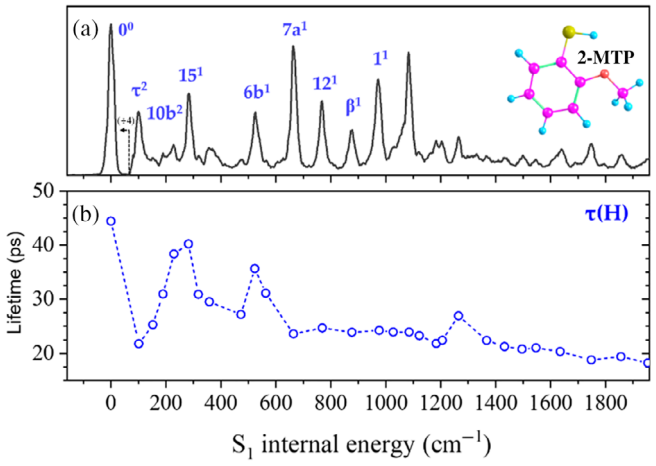

FIGURE 6 (a) Picosecond (1 + 1′) resonance-enhanced two-photon ionization (R2PI) spectrum of the S_1 state 2-methoxythiophenol (2-MTP) with the vibronic band assignment.[93] (b) Plot of the S_1 state lifetimes of 2-MTP obtained from the parent ion transients and single-exponential fits

confirming that the S—H bond dissociation takes place via tunneling. Most dramatically, the tunneling rate of 2-MTP increases approximately twofold when exciting the τ_{MeO2} (101 cm^{-1}) or $10b^2$ (152 cm^{-1}) out-of-plane modes, giving corresponding lifetimes of ~22 or 25 ps, respectively, before falling back to $\tau \approx 40$ ps at the 15^1 (282 cm^{-1}) mode excitation. Thereafter, the tunneling rate increases rather monotonically with increasing the internal energy. The multidimensional nature of the tunneling dynamics should be invoked for the explanation of the experiment. For instance, the $10b^2$ (152 cm^{-1}) mode involves the dihedral torsional motion of the S—H bond with respect to the molecular plane. In a two-dimensional picture involving the S—H bond elongation (parallel to the gradient vector) and out-of-plane torsional angle (parallel to the coupling vector) coordinates, the S_1/S_2 conical intersection appears as an apex at the planar geometry, with lower-lying saddle points along the S—H out-of-plane torsional coordinate. In this case, the lower S_1 adiabatic potential energy surface laid along the S—H out-of-plane torsional angle is dynamically "shaped" by the upper-lying S_1/S_2 conical intersection. As the minimum energy geometry of the S_1 2-MTP is pseudo-planar, the reactive flux prepared at the τ_{MeO2} or $10b^2$ mode excitation is supposed to follow the tunneling path through the adiabatic barrier which has been much reduced along the associated out-of-plane coupling vectors at the conical intersection. This is the direct consequence of the "shaping" of the multidimensional tunneling barrier mediated by the coupling vectors at the conical intersection seam.

The picosecond time-resolved transient at the S_1 origin of 2-FTP gives the tunneling lifetime of ≈12.3 ps. Quite similar to the case of 2-MTP, it is abruptly reduced to $\tau \approx 6.0$ ps at the $10b^2$ (155 cm^{-1}) mode excitation whereas it sharply increases again to $\tau \approx 12$ ps at the in-plane 15^1 (235 cm^{-1}) mode excitation. Though it is less dramatic, the mode-specific fluctuation of tunneling rates of 2-FTP continues up to the S_1 internal energy of ~1000 cm^{-1}. Thereafter, the tunneling rate increases monotonically, indicating that the energy randomization process starts to overwhelm in the higher internal energy region. The S_1 state lifetime with increasing internal energy found for 2-CTP is somewhat different to that in 2-FTP and 2-MTP. The lifetime of the S_1 origin of 2-CTP is ~227 ps. The acceleration of the tunneling process by the out-of-plane mode excitation ($\tau \sim 104$ ps at the $10b^2$ [195 cm^{-1}] mode excitation) is also quite evident in 2-CTP, confirming again that the tunneling dynamics is dictated by the upper-lying conical intersection along the out-of-plane S—H torsional angle. However, the S_1 lifetime of 2-CTP thereafter decreases very rapidly with increasing the S_1 internal energy, giving $\tau \sim 60$ or 11 ps at ~600 or 1100 cm^{-1}, respectively. Such a rapid change of the S_1 decaying rate suggests that the fast nonradiative decay channel should be newly opened at the low internal energies. Nonradiative transitions through the near-lying conical intersection mediated by the C—Cl bond extension and/or HCl formation coordinate might be responsible for the fast S_1 decaying channel of 2-CTP. The similar phenomenon of the ultrafast excited-state decay has also been observed in the S_1 dynamics of 2-chlorophenol (see Section 2.2).[147,152] The strong S—H···Cl (2-CTP) or O—H···Cl (2-chlorophenol) intramolecular hydrogen bonding as well as the presence of the πσ* state along the C_2—Cl bond extension coordinate seem to be responsible for the ultrafast nonradiative transitions (other than the H-atom tunneling) in those systems. Although it might be complicated, the peculiar dynamic behavior of 2-chlorophenol or 2-chlorothiophenol brings another very interesting issue in photochemistry.

Quite intriguing finding is that the Autler–Townes (AT) splitting has been experimentally observed in all of 2-MTP, 2-FTP, and 2-CTP in the nanosecond R2PI spectroscopy.[97] Actually, the AT splitting has not been anticipated as there are many internal degrees of freedom, and thus it has long been considered that it should be negligible in the spectroscopy of polyatomic molecules. Surprisingly, however, the AT splitting has been clearly observed for all *ortho*-substituted thiophenols especially between zero-point levels of S_0 and S_1, allowing the direct observation of the light-dressed states in polyatomic molecules. Remarkably, AT splitting is found to be robust if the coherent Rabi frequency and dephasing dynamics of the coupled eigenstates are within certain ranges even for polyatomic molecules, especially if they provide the open system of which the excited-state lifetime is shorter than hundreds of picoseconds. The semi-classical optical Bloch equations[160] or the dressed-atom approach[161] based on the three-state atomic level model are found to be extremely useful for the successful explanation of the experiment.[97] Generally speaking, the AT split energy gap increases as the state S_1 lifetime decreases. The plot of AT

splitting versus the square root of the laser intensity for all three molecules (2-MTP, 2-FTP, and 2-CTP) shows a straight line. As the molecule becomes more complicated, the atomic model seems to be less validated. Therefore, the influence of the complexity on the state dressing is a remaining subject to be resolved.

THE O—H BOND TUNNELING IN THE S_1 STATES OF BENZENEDIOLS AND THEIR WATER CLUSTERS

The S_1 excited-state dynamics of three different benzenediols such as catechol (1,2-dihyroxybenzene), resorcinol (1,3-dihydroxybenzene), and hydroquinone (1,4-dihyroxybenzene) as well as their 1:1 water clusters have been investigated.[151] The state-specific S_1 lifetime of catechol was reported to be 7 or 11 ps at the S_1 origin and first quantum of the OH torsional mode, respectively,[117,118,148] and it has been ascribed to the nonplanarity of the S_1 catechol at its minimum energy.[162,163] The S_1 lifetime of hydroquinone had been reported to be 2.7–3.0 ns,[145,148,149] whereas that of resorcinol seems to be scattered in the literature, giving the lifetime in the 2.7–4.5 ns range.[143,145,148,149] When benzenediols are complexed with a single water molecule, the S_1 relaxation dynamics is significantly influenced by the modified potential energy surfaces especially in the vicinity of the $\pi\pi^*/\pi\sigma^*$ curve crossing regions.[148,149] Recently, the state-specific S_1 lifetimes of three benzenediols at various vibronic levels have been precisely measured using the narrow-band picosecond laser pulses ($\Delta E \sim 20$ cm–1 and $\Delta t \sim 1.7$ ps), giving state- and/or conformer-specific S_1 decaying lifetimes.[151] In addition, the S_1-state lifetimes of 1:1 clusters of water with catechol, resorcinol, and hydroquinone are also estimated in a conformer-specific way.

The picosecond ($1 + 1'$) R2PI spectrum of the jet-cooled catechol shows distinct S_1 vibronic structures (Figure 7) where each vibronic band is appropriately assigned. The lifetime (τ) at the zero-point level (0^0) is ~5.9 ps, and it increases to $\tau \sim 9.0$ ps at the 116 cm^{-1} band (the first symmetry-allowed OH out-of-plane torsional mode [τ^1]) while it slightly decreases to $\tau \sim 7.9$ ps at the 257 cm^{-1} band (τ^2). This is due to the dynamic change of the tunneling barrier, indicating that the $S_1(\pi\pi^*)/S_2(\pi\sigma^*)$ conical intersection is avoided more efficiently at the nonplanar geometry to lower the effective tunneling barrier for the H-atom detachment. This is in accordance with the experimental studies on the tunneling dynamics of 2-MTP, 2-FTP, and 2-CTP as described in Section 3.2. The catechol·water 1:1 cluster has the minimum energy structure where the free OH moiety is hydrogen-bonded with the water molecule in both ground (S_0) and excited (S_1) electronic states.[164,165] The picosecond R2PI spectrum of the catechol·water cluster identifies the S_1 origin band which is red-shifted from that of the monomer by ~150 cm^{-1}.[164] At its zero-point energy (ZPE) level, the S_1 lifetime of the cluster is estimated to be ~1.8–2.0 ns.[148,151] The 300-fold retardation of the S_1 decay rate by the water clustering could be due to the huge increase of the reaction barrier against the H-atom detachment or the excited-state hydrogen transfer (ESHT) process,[1] indicating that the H-atom detachment reaction is completely blocked in the cluster. The nonradiative transitions such as the internal conversion or intersystem crossing should be largely responsible for the rather slow decaying time of the S_1 state of the catechol·water cluster. Interestingly, the S_1 lifetime gets significantly shortened to $\tau \sim 1.03$ ns at the intermolecular stretching mode (σ) excitation at 146 cm^{-1}, suggesting that the ESHT through the intermolecular hydrogen bonding might take place (Figure 7).[38,116,166–168]

The S_1 lifetime of the C_S asymmetric isomer (*cis*) or C_{2V} symmetric isomer (*trans*) of resorcinol has been estimated to be ~4.5 or 6.3 ns at its ZPE, respectively. Although the lifetime of *trans* is about 1.4 times longer than *cis*, the lifetime estimation is subject to the further refinement as the reported lifetimes are rather scattered in literatures[143,145,148,149] and the experimental temporal window was limited to 0–2.7 ns. The relatively long S_1 lifetime of both conformers of resorcinol suggests that the nonadiabatic transition may be more responsible for the S_1 relaxation process compared to the H-atom detachment.[143] The resorcinol·water (1:1) clusters give slightly shorter S_1 lifetimes compared to those of monomers, giving $\tau \sim 3.0$–4.5 ns, indicating that the S_1 lifetime gets shortened by the 1:1 clustering with water. For hydroquinone, the S_1 lifetime turns out to be not conformer-specific, giving $\tau \sim 2.8$ ns for both *trans* and *cis* conformers. Spectroscopic identification of *trans* and *cis* conformers of hydroquinone and their water clusters had been well established by the recent Stark deflection experiment,[169] where the differences in dipole moments of different conformers have been utilized for the spatial deflection in the strong electric field, giving the unambiguous identification of the structural isomers of hydroquinone and its water clusters. The S_1 decay is facilitated by the water clustering for both *trans* and *cis* of hydroquinone, giving $\tau \sim 2.27$ or 1.92 ns, respectively, which is attributed to the electron-withdrawing effect of hydrogen-bonded water on the OH moiety in the *para* position with respect to the free OH moiety undergoing the H-atom detachment via tunneling. In contrast to the case of the catechol·water cluster, the intramolecular hydrogen-bond stretching mode (σ) does not seem to play the significant role in the tunneling rate of the hydroquinone·water cluster, implying that ESHT may not be activated in the latter due to the much higher potential barrier of hydroquinone. Ab initio calculations support the experiment quite well.[151]

SUMMARY AND OUTLOOK

The $\pi\sigma^*$-mediated photochemistry has been intensively studied for many years. The dynamic role of the $\pi\sigma^*$ state through the vibronic coupling to the nearby

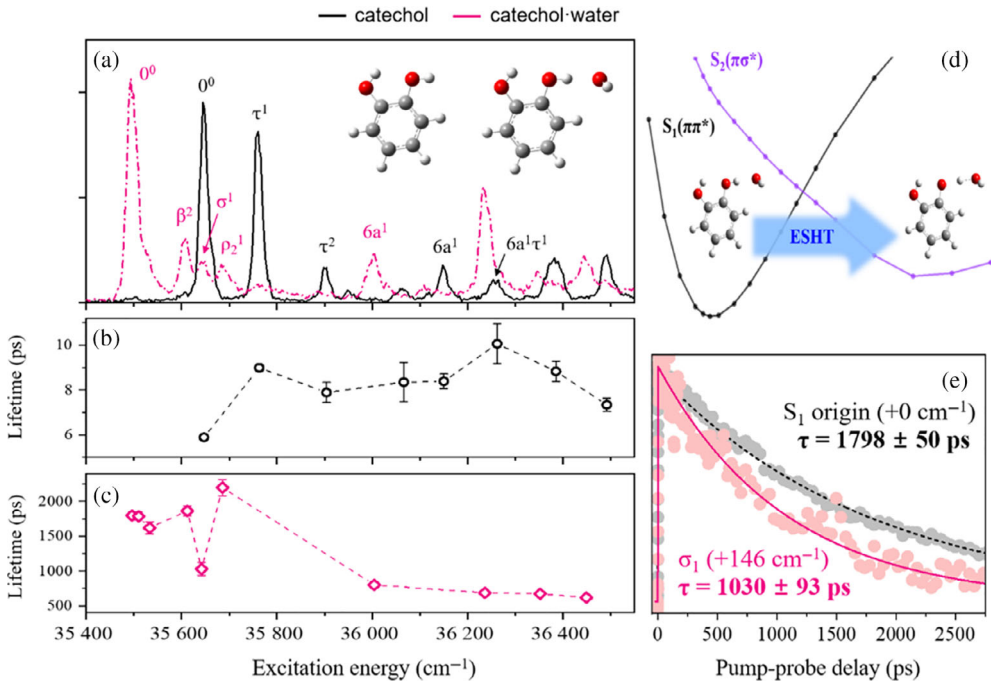

FIGURE 7 (a) Picosecond (1 + 1′) resonance-enhanced two-photon ionization (R2PI) spectra of catechol (black) and the catechol·water cluster (magenta) with the vibronic band assignment.[164] Mode-specific S_1 lifetimes of (b) catechol and (c) the catechol·water cluster obtained by monitoring the parent ion signal as a function of pump-probe time delay. (d,e) The S_1 lifetime of the catechol·water cluster gets shortened by twofold at the intramolecular hydrogen bond stretching vibrational mode (σ) excitation, implying that the excited state hydrogen transfer (ESHT) might occur through the reaction barrier under the S_1/S_2 curve crossing

optically bright ππ* state turns out to be quite essential in understanding (and controlling) the excited-state chemistry of heteroaromatic polyatomic systems. Ultrafast energy transfer and/or relaxation among different vibronic states which plays an important role in protecting the biological system from the external irradiation take place via the nonadiabatic coupling to the πσ* state,[1] for example. Curve-crossings of the bound ππ* state (S_1) and the unbound πσ* state (S_2) give rise to the conical intersections along many different relaxation pathways, provoking the scientific investigation of the nonadiabatic dynamics in the vicinity of the conical intersection. Especially, as the conical intersections encountered along the various reaction paths are multidimensional in nature, the excited-state chemistry of the heteroaromatic systems provides the great opportunity to study the multiple aspects of the conical intersection in terms of its structure and dynamic role. Although the optical window is often Franck–Condon limited, the various vibronic mode excitations could prepare the reactive fluxes spanning many different nuclear configurations where nonadiabatic dynamics is dictated depending on their degrees of the proximity to the conical intersection. In the same context, the adiabatic potential energy surfaces are dynamically shaped by the upper-lying conical intersection extended along the multidimensional seam coordinates, governing the rate and energy disposal dynamics associated with predissociation, tunneling, or other nonradiative transition processes. In this regard, the study of the H-atom tunneling reactions in the S_1 states of phenols or thiophenols (as reviewed in this article) are quite meaningful as one can study the new aspects of the dynamic shaping of the tunneling barrier by the presence of the upper-lying conical intersection. The state-specific tunneling rates of phenols and thiophenols, measured by the picosecond time-resolved pump-probe scheme, reveal their drastic mode-dependences, confirming the multidimensionality of the tunneling dynamics. The excitations of the low-frequency (particularly out-of-plane) vibrational modes are found to be enormously influential on the tunneling rate, indicating that such vibrational modes (which are completely orthogonal to the O—H (or S—H) bond extension coordinate) are actually quite critical in the dynamic shaping of the adiabatic potential energy surfaces. Control of the tunneling dynamics by the nuclear layout along the seam coordinate of the conical intersection has been nicely demonstrated in the O—H tunneling reaction of the *trans-o*-cresol (Figure 8). The (effective) tunneling barrier is modulated by the CH_3 internal rotor states, and its effect on the tunneling dynamics has been clearly manifested in the sharply varying state-specific tunneling rates. This is a beautiful demonstration of the dynamic shaping of the tunneling barrier by the upper-lying conical intersection extended along the particular normal mode

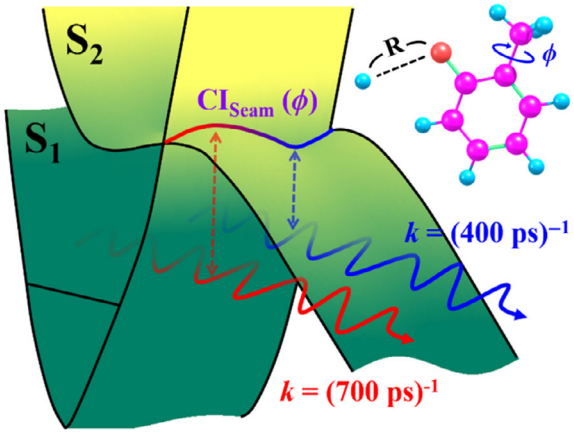

FIGURE 8 The role of the conical intersection extended along the seam coordinate in dictating the tunneling dynamics through the underneath barrier (adapted from Ref. 121)

coordinate which is absolutely orthogonal to the reaction coordinate.

Phenols and thiophenols are similar in the overall characteristics of the excited-state photochemistry in general. And yet, they are quite different in terms of the structures, energetics and resultant dynamic details. Especially, thiophenols are found to be the ideal systems to interrogate the nonadiabatic transition dynamics, as it is plausible to quantify the nonadiabatic transition probability with changing the quantum variables of the reactive flux. For instance, as the nonadiabatic transition probability is (qualitatively) proportional to the proximity degree of the reactive flux to the conical intersection, its structure could be informed by identifying the nuclear configuration spanned by the particular reactive flux which gives the higher nonadiabatic transition probability. Though the underlying principles behind the dynamic behaviors of phenols or thiophenols would remain not much different, the individual systems have their own characteristics. For instance, the S_1-state dynamics of 2-chlorophenol or 2-chlorothiophenol is very interesting as the ultrafast nonradiative transition process competes with the H-atom tunneling and it seems to be mediated by the strong intramolecular hydrogen bonding. Generally speaking, it is still quite a formidable task to figure out the structure and dynamic role of the conical intersection of the polyatomic molecules. As the optical excitation is governed by the Franck–Condon principle, the complete characterization of the conical intersection in the multidimensional coordinates is not unambiguous yet. In the high-frequency region, the energy randomization rate becomes comparable to or exceeds the tunneling rate in many cases. Therefore, it is not feasible to unravel the mode-specific dynamics along the high-frequency normal mode coordinates. In order to overcome these difficulties, one may employ the infrared + ultraviolet double excitation schemes to explore the otherwise inaccessible nuclear configurations of the excited state. The harsh cooling of the sample lower than 0.1 K may help to reduce the IVR rate in the high internal energy region. The experimental observation of the geometric phase for the reactive fluxes encircling the conical intersection seems to be a quite challenging remaining issue. Measurement of the tunneling rates for a series of the overtones of the identical vibrational mode might be extremely interesting as it could show the modulation of the tunneling rate due to the constructive or destructive interferences caused by the geometric phase. Theoretical modeling for the explanation of the tunneling experiment is highly desirable in the near future. The one-dimensional semiclassical WKB approximation is anticipated to be not satisfactory. The Zhu–Nakamura (ZN) theory developed based on the semi-classical nonadiabatic model might be quite helpful for the more quantitative comparison with the experiment as the concept of the nonadiabatic coupling has been invoked in the ZN theory.[170–174] Full quantum mechanical calculations would be quite desirable though they are quite demanding as the full-dimensional potential energy surfaces of polyatomic molecular systems are required.

ACKNOWLEDGMENT

This work was supported by the National Research Foundation of Korea (2018R1A2B3004534, 2019K1A3A1A14064258, and 2019R1A6A1A10073887).

CONFLICT OF INTEREST

The authors declare no potential conflict of interest.

ORCID

Junggil Kim https://orcid.org/0000-0002-9027-1546
Kyung Chul Woo https://orcid.org/0000-0002-9387-9397
Sang Kyu Kim https://orcid.org/0000-0003-4803-1327

REFERENCES

[1] A. L. Sobolewski, W. Domcke, C. Dedonder-Lardeux, C. Jouvet, *Phys. Chem. Chem. Phys.* **2002**, *4*, 1093.
[2] W. Domcke, A. L. Sobolewski, *Science* **2003**, *302*, 1693.
[3] M. N. R. Ashfold, B. Cronin, A. L. Devine, R. N. Dixon, M. G. D. Nix, *Science* **2006**, *312*, 1637.
[4] M. N. R. Ashfold, G. A. King, D. Murdock, M. G. D. Nix, T. A. A. Oliver, A. G. Sage, *Phys. Chem. Chem. Phys.* **2010**, *12*, 1218.
[5] G. M. Roberts, D. J. Hadden, L. T. Bergendahl, A. M. Wenge, S. J. Harris, T. N. V. Karsili, M. N. R. Ashfold, M. J. Paterson, V. G. Stavros, *Chem. Sci.* **2013**, *4*, 993.
[6] G. M. Roberts, V. G. Stavros, *Chem. Sci.* **2014**, *5*, 1698.
[7] H. S. You, S. Han, J.-H. Yoon, J. S. Lim, J. Lee, S.-Y. Kim, D.-S. Ahn, J. S. Lim, S. K. Kim, *Int. Rev. Phys. Chem.* **2015**, *34*, 429.
[8] M. N. R. Ashfold, D. Murdock, T. A. A. Oliver, *Annu. Rev. Phys. Chem.* **2017**, *68*, 63.
[9] Z. Lan, W. Domcke, V. Vallet, A. L. Sobolewski, S. Mahapatra, *J. Chem. Phys.* **2005**, *122*, 224315.
[10] I. S. Lim, J. S. Lim, Y. S. Lee, S. K. Kim, *J. Chem. Phys.* **2007**, *126*, 034306.
[11] J. S. Lim, Y. S. Lee, S. K. Kim, *Angew. Chem., Int. Ed.* **2008**, *47*, 1853.
[12] M. N. R. Ashfold, A. L. Devine, R. N. Dixon, G. A. King, M. G. D. Nix, T. A. A. Oliver, *Proc. Natl. Acad. Sci.* **2008**, *105*, 12701.
[13] L. J. Butler, *Annu. Rev. Phys. Chem.* **1998**, *49*, 125.
[14] G. A. Worth, L. S. Cederbaum, *Annu. Rev. Phys. Chem.* **2004**, *55*, 127.
[15] T.-S. Chu, Y. Zhang, K.-L. Han, *Int. Rev. Phys. Chem.* **2006**, *25*, 201.

[16] J. C. Tully, *J. Chem. Phys.* **2012**, *137*, 22A301.
[17] D. R. Yarkony, *Chem. Rev.* **2012**, *112*, 481.
[18] W. Domcke, D. R. Yarkony, *Annu. Rev. Phys. Chem.* **2012**, *63*, 325.
[19] F. Bernardi, M. Olivucci, M. A. Robb, *Chem. Soc. Rev.* **1996**, *25*, 321.
[20] R. W. Schoenlein, L. A. Peteanu, R. A. Mathies, C. V. Shank, *Science* **1991**, *254*, 412.
[21] H. Kang, K. T. Lee, B. Jung, Y. J. Ko, S. K. Kim, *J. Am. Chem. Soc.* **2002**, *124*, 12958.
[22] C. Ko, B. Levine, A. Toniolo, L. Manohar, S. Olsen, H.-J. Werner, T. J. Martinez, *J. Am. Chem. Soc.* **2003**, *125*, 12710.
[23] S. Ullrich, T. Schultz, M. Z. Zgierski, A. Stolow, *Phys. Chem. Chem. Phys.* **2004**, *6*, 2796.
[24] H. Satzger, D. Townsend, M. Z. Zgierski, S. Patchkovskii, S. Ullrich, A. Stolow, *Proc. Natl. Acad. Sci.* **2006**, *103*, 10196.
[25] S. Yamazaki, W. Domcke, A. L. Sobolewski, *J. Phys. Chem. A* **2008**, *112*, 11965.
[26] M. Barbatti, H. Lischka, S. Salzmann, C. M. Marian, *J. Chem. Phys.* **2009**, *130*, 034305.
[27] T. Horio, T. Fuji, Y.-I. Suzuki, T. Suzuki, *J. Am. Chem. Soc.* **2009**, *131*, 10392.
[28] D. Asturiol, B. Lasorne, G. A. Worth, M. A. Robb, L. Blancafort, *Phys. Chem. Chem. Phys.* **2010**, *12*, 4949.
[29] Q. Li, L. Blancafort, *Photochem. Photobiol. Sci.* **2013**, *12*, 1401.
[30] M. Malis, Y. Loquais, E. Gloaguen, C. Jouvet, V. Brenner, M. Mons, I. Ljubic, N. Doslic, *Phys. Chem. Chem. Phys.* **2014**, *16*, 2285.
[31] D. Polli, O. Weingart, D. Brida, E. Poli, M. Maiuri, K. M. Spillane, A. Bottoni, P. Kukura, R. A. Mathies, G. Cerullo, M. Garavelli, *Angew. Chem., Int. Ed.* **2014**, *53*, 2504.
[32] C. E. Crespo-Hernandez, L. Martinez-Fernandez, C. Rauer, C. Reichardt, S. Mai, M. Pollum, P. Marquetand, L. Gonzalez, I. Corral, *J. Am. Chem. Soc.* **2015**, *137*, 4368.
[33] L. A. Baker, B. Marchetti, T. N. V. Karsili, V. G. Stavros, M. N. R. Ashfold, *Chem. Soc. Rev.* **2017**, *46*, 3770.
[34] M. N. R. Ashfold, M. Bain, C. S. Hansen, R. A. Ingle, T. N. V. Karsili, B. Marchetti, D. Murdock, *J. Phys. Chem. Lett.* **2017**, *8*, 3440.
[35] R. Losantos, I. Lamas, R. Montero, A. Longarte, D. Sampedro, *Phys. Chem. Chem. Phys.* **2019**, *21*, 11376.
[36] S. Soorkia, C. Jouvet, G. Gregoire, *Chem. Rev.* **2020**, *120*, 3296.
[37] L. Grisanti, M. Sapunar, A. Hassanali, N. Doslic, *J. Am. Chem. Soc.* **2020**, *142*, 18042.
[38] C. Jouvet, M. Miyazaki, M. Fujii, *Chem. Sci.* **2021**, *12*, 3836.
[39] A. L. Sobolewski, W. Domcke, *J. Phys. Chem. A* **2001**, *105*, 9275.
[40] C. M. Tseng, Y. T. Lee, C. K. Ni, *J. Chem. Phys.* **2004**, *121*, 2459.
[41] M. G. D. Nix, A. L. Devine, B. Cronin, R. N. Dixon, M. N. R. Ashfold, *J. Chem. Phys.* **2006**, *125*, 133318.
[42] M. Abe, Y. Ohtsuki, Y. Fujimura, Z. Lan, W. Domcke, *J. Chem. Phys.* **2006**, *124*, 224316.
[43] C.-M. Tseng, Y. T. Lee, M.-F. Lin, C.-K. Ni, S.-Y. Liu, Y.-P. Lee, Z. F. Xu, M. C. Lin, *J. Phys. Chem. A* **2007**, *111*, 9463.
[44] M. G. D. Nix, A. L. Devine, R. N. Dixon, M. N. R. Ashfold, *Chem. Phys. Lett.* **2008**, *463*, 305.
[45] A. Iqbal, L.-J. Pegg, V. G. Stavros, *J. Phys. Chem. A* **2008**, *112*, 9531.
[46] O. P. Vieuxmaire, Z. Lan, A. L. Sobolewski, W. Domcke, *J. Chem. Phys.* **2008**, *129*, 224307.
[47] M. L. Hause, Y. Heidi Yoon, A. S. Case, F. F. Crim, *J. Chem. Phys.* **2008**, *128*, 104307.
[48] G. A. King, T. A. A. Oliver, M. G. D. Nix, M. N. R. Ashfold, *J. Phys. Chem. A* **2009**, *113*, 7984.
[49] A. Iqbal, M. S. Y. Cheung, M. G. D. Nix, V. G. Stavros, *J. Phys. Chem. A* **2009**, *113*, 8157.
[50] R. N. Dixon, T. A. A. Oliver, M. N. R. Ashfold, *J. Chem. Phys.* **2011**, *134*, 194303.
[51] H. An, K. K. Baeck, *J. Phys. Chem. A* **2011**, *115*, 13309.
[52] Y. Zhang, T. A. A. Oliver, M. N. R. Ashfold, S. E. Bradforth, *Faraday Discuss.* **2012**, *157*, 141.
[53] G. M. Roberts, A. S. Chatterley, J. D. Young, V. G. Stavros, *J. Phys. Chem. Lett.* **2012**, *3*, 348.
[54] R. A. Livingstone, J. O. Thompson, M. Iljina, R. J. Donaldson, B. J. Sussman, M. J. Paterson, D. Townsend, *J. Chem. Phys.* **2012**, *137*, 184304.
[55] S. G. Ramesh, W. Domcke, *Faraday Discuss.* **2013**, *163*, 73.
[56] X. Xu, K. R. Yang, D. G. Truhlar, *J. Chem. Theory Comput.* **2013**, *9*, 3612.
[57] X. Zhu, D. R. Yarkony, *J. Chem. Phys.* **2014**, *140*, 024112.
[58] K. R. Yang, X. F. Xu, J. J. Zheng, D. G. Truhlar, *Chem. Sci.* **2014**, *5*, 4661.
[59] X. Xu, J. Zheng, K. R. Yang, D. G. Truhlar, *J. Am. Chem. Soc.* **2014**, *136*, 16378.
[60] X. Zhu, D. R. Yarkony, *J. Chem. Phys.* **2016**, *144*, 024105.
[61] X. Zhu, C. L. Malbon, D. R. Yarkony, *J. Chem. Phys.* **2016**, *144*, 124312.
[62] H. Guo, D. R. Yarkony, *Phys. Chem. Chem. Phys.* **2016**, *18*, 26335.
[63] C. Xie, J. Ma, X. Zhu, D. R. Yarkony, D. Xie, H. Guo, *J. Am. Chem. Soc.* **2016**, *138*, 7828.
[64] C. Xie, C. L. Malbon, D. R. Yarkony, H. Guo, *J. Chem. Phys.* **2017**, *147*, 044109.
[65] C. Xie, H. Guo, *Chem. Phys. Lett.* **2017**, *683*, 222.
[66] W. Xie, W. Domcke, *J. Chem. Phys.* **2017**, *147*, 184114.
[67] K. Rajak, A. Ghosh, S. Mahapatra, *J. Chem. Phys.* **2018**, *148*, 054301.
[68] Y.-C. Lin, C. Lee, S.-H. Lee, Y.-Y. Lee, Y. T. Lee, C.-M. Tseng, C.-K. Ni, *J. Chem. Phys.* **2018**, *148*, 074306.
[69] H. Y. Lai, W. R. Jhang, C.-M. Tseng, *J. Chem. Phys.* **2018**, *149*, 031104.
[70] Y. He, H. Zhao, W. Wang, *Int. J. Quantum Chem.* **2018**, *118*, e25786.
[71] C. Xie, C. L. Malbon, H. Guo, D. R. Yarkony, *Acc. Chem. Res.* **2019**, *52*, 501.
[72] K. I. Hilsabeck, J. L. Meiser, M. Sneha, J. A. Harrison, R. N. Zare, *J. Am. Chem. Soc.* **2019**, *141*, 1067.
[73] K. C. Woo, S. K. Kim, *J. Phys. Chem. A* **2019**, *123*, 1529.
[74] C. Xie, B. Zhao, C. L. Malbon, D. R. Yarkony, D. Xie, H. Guo, *J. Phys. Chem. Lett.* **2020**, *11*, 191.
[75] G. Christopoulou, T. Tran, G. A. Worth, *Phys. Chem. Chem. Phys.* **2021**, *23*, 23684.
[76] J. S. Lim, I. S. Lim, K.-S. Lee, D.-S. Ahn, Y. S. Lee, S. K. Kim, *Angew. Chem., Int. Ed.* **2006**, *45*, 6290.
[77] J. S. Lim, H. Choi, I. S. Lim, S. B. Park, Y. S. Lee, S. K. Kim, *J. Phys. Chem. A* **2009**, *113*, 10410.
[78] A. L. Devine, M. G. D. Nix, R. N. Dixon, M. N. R. Ashfold, *J. Phys. Chem. A* **2008**, *112*, 9563.
[79] T. A. A. Oliver, Y. Zhang, M. N. R. Ashfold, S. E. Bradforth, *Faraday Discuss.* **2011**, *150*, 439.
[80] T. A. A. Oliver, G. A. King, D. P. Tew, R. N. Dixon, M. N. R. Ashfold, *J. Phys. Chem. A* **2012**, *116*, 12444.
[81] T. S. Venkatesan, S. G. Ramesh, Z. Lan, W. Domcke, *J. Chem. Phys.* **2012**, *136*, 174312.
[82] H. An, H. Choi, Y. S. Lee, K. K. Baeck, *ChemPhysChem* **2015**, *16*, 1529.
[83] H. S. You, S. Han, J. S. Lim, S. K. Kim, *J. Phys. Chem. Lett.* **2015**, *6*, 3202.
[84] I. Reva, M. J. Nowak, L. Lapinski, R. Fausto, *Phys. Chem. Chem. Phys.* **2015**, *17*, 4888.
[85] V. Ovejas, M. Fernandez-Fernandez, R. Montero, A. Longarte, *Chem. Phys. Lett.* **2016**, *661*, 206.
[86] B. Marchetti, T. N. V. Karsili, M. Cipriani, C. S. Hansen, M. N. R. Ashfold, *J. Chem. Phys.* **2017**, *147*, 013923.
[87] G.-S.-M. Lin, C. Xie, D. Xie, *J. Phys. Chem. A* **2017**, *121*, 8432.
[88] G.-S.-M. Lin, C. Xie, D. Xie, *J. Phys. Chem. A* **2018**, *122*, 5375.
[89] L. Zhang, D. G. Truhlar, S. Sun, *Phys. Chem. Chem. Phys.* **2018**, *20*, 28144.
[90] L. Zhang, D. G. Truhlar, S. Sun, *J. Chem. Phys.* **2019**, *151*, 154306.
[91] D. Cho, J. R. Rouxel, S. Mukamel, *J. Phys. Chem. Lett.* **2020**, *11*, 4292.
[92] M. Hayashi, R. Ichihara, N. Akai, M. Nakata, *J. Mol. Struct.* **2021**, *1244*, 130909.
[93] S. Han, H. S. You, S.-Y. Kim, S. K. Kim, *J. Phys. Chem. A* **2014**, *118*, 6940.

[94] J. S. Lim, H. S. You, S. Han, S. K. Kim, *J. Phys. Chem. A* **2019**, *123*, 2634.
[95] J. S. Lim, H. S. You, S.-Y. Kim, J. Kim, Y. C. Park, S. K. Kim, *J. Chem. Phys.* **2019**, *151*, 244305.
[96] K. C. Woo, S. K. Kim, *J. Phys. Chem. Lett.* **2020**, *11*, 6730.
[97] J. Kim, J. S. Lim, H.-R. Noh, S. K. Kim, *J. Phys. Chem. Lett.* **2020**, *11*, 6791.
[98] C.-M. Tseng, Y. T. Lee, C.-K. Ni, *J. Phys. Chem. A* **2009**, *113*, 3881.
[99] D. J. Hadden, C. A. Williams, G. M. Roberts, V. G. Stavros, *Phys. Chem. Chem. Phys.* **2011**, *13*, 4494.
[100] D. J. Hadden, G. M. Roberts, T. N. V. Karsili, M. N. R. Ashfold, V. G. Stavros, *Phys. Chem. Chem. Phys.* **2012**, *14*, 13415.
[101] R. Omidyan, H. Rezaei, *Phys. Chem. Chem. Phys.* **2014**, *16*, 11679.
[102] A. Shastri, A. K. Das, B. N. Rajasekhar, *J. Quant. Spectrosc. Radiat. Trans.* **2020**, *242*, 106782.
[103] J. S. Lim, S. K. Kim, *Nat. Chem.* **2010**, *2*, 627.
[104] S. Han, J. S. Lim, J.-H. Yoon, J. Lee, S.-Y. Kim, S. K. Kim, *J. Chem. Phys.* **2014**, *140*, 054307.
[105] S. L. Li, X. Xu, D. G. Truhlar, *Phys. Chem. Chem. Phys.* **2015**, *17*, 20093.
[106] S.-Y. Kim, J. Lee, S. K. Kim, Y. S. Choi, *Chem. Phys. Lett.* **2016**, *659*, 43.
[107] S.-Y. Kim, J. Lee, S. K. Kim, *Phys. Chem. Chem. Phys.* **2017**, *19*, 18902.
[108] K. C. Woo, D. H. Kang, S. K. Kim, *J. Am. Chem. Soc.* **2017**, *139*, 17152.
[109] S. L. Li, D. G. Truhlar, *J. Chem. Phys.* **2017**, *146*, 064301.
[110] S. L. Li, D. G. Truhlar, *J. Chem. Phys.* **2017**, *147*, 044311.
[111] Y. Shu, D. G. Truhlar, *Chem. Phys.* **2018**, *515*, 737.
[112] J. S. Lim, H. S. You, S.-Y. Kim, S. K. Kim, *Chem. Sci.* **2019**, *10*, 2404.
[113] H. Lee, S.-Y. Kim, J. S. Lim, J. Kim, S. K. Kim, *J. Phys. Chem. A* **2020**, *124*, 4666.
[114] H. Lee, S.-Y. Kim, S. K. Kim, *Chem. Sci.* **2020**, *11*, 6856.
[115] J. Kim, K. C. Woo, S. K. Kim, *J. Phys. Chem. A* **2021**, *125*, 6629.
[116] G. A. Pino, A. N. Oldani, E. Marceca, M. Fujii, S.-I. Ishiuchi, M. Miyazaki, M. Broquier, C. Dedonder, C. Jouvet, *J. Chem. Phys.* **2010**, *133*, 124313.
[117] M. Weiler, M. Miyazaki, G. Feraud, S.-I. Ishiuchi, C. Dedonder, C. Jouvet, M. Fujii, *J. Phys. Chem. Lett.* **2013**, *4*, 3819.
[118] A. S. Chatterley, J. D. Young, D. Townsend, J. M. Zurek, M. J. Paterson, G. M. Roberts, V. G. Stavros, *Phys. Chem. Chem. Phys.* **2013**, *15*, 6879.
[119] M. C. Capello, M. Broquier, S.-I. Ishiuchi, W. Y. Sohn, M. Fujii, C. Dedonder-Lardeux, C. Jouvet, G. A. Pino, *J. Phys. Chem. A.* **2014**, *118*, 2056.
[120] X. Deng, Y. Tang, X. Song, K. Liu, Z. Gu, B. Zhang, *Chemosphere* **2020**, *253*, 126747.
[121] K. C. Woo, J. Kim, S. K. Kim, *J. Phys. Chem. Lett.* **2021**, *12*, 1854.
[122] O. Tishchenko, D. G. Truhlar, A. Ceulemans, M. T. Nguyen, *J. Am. Chem. Soc.* **2008**, *130*, 7000.
[123] A. Sur, P. M. Johnson, *J. Chem. Phys.* **1986**, *84*, 1206.
[124] R. J. Lipert, G. Bermudez, S. D. Colson, *J. Phys. Chem.* **1988**, *92*, 3801.
[125] G. Berden, W. L. Meerts, *J. Chem. Phys.* **1996**, *104*, 972.
[126] G. Gregoire, C. Dedonder-Lardeux, C. Jouvet, S. Martrenchard, D. Solgadi, *J. Phys. Chem. A* **2001**, *105*, 5971.
[127] C. Ratzer, J. Kupper, D. Spangenberg, M. Schmitt, *Chem. Phys.* **2002**, *283*, 153.
[128] R. J. Lipert, S. D. Colson, *J. Phys. Chem.* **1989**, *93*, 135.
[129] C. Lee, Y.-C. Lin, S.-H. Lee, Y.-Y. Lee, C.-M. Tseng, Y.-T. Lee, C.-K. Ni, *J. Chem. Phys.* **2017**, *147*, 013904.
[130] A. S. Chatterley, G. M. Roberts, V. G. Stavros, *J. Chem. Phys.* **2013**, *139*, 034318.
[131] C. Xie, D. R. Yarkony, H. Guo, *Phys. Rev. A* **2017**, *95*, 022104.
[132] C. Xie, B. K. Kendrick, D. R. Yarkony, H. Guo, *J. Chem. Theory Comput.* **2017**, *13*, 1902.
[133] K. C. Woo, S. K. Kim, *J. Phys. Chem. Lett.* **2020**, *11*, 161.
[134] H. D. Bist, J. C. D. Brand, D. R. Williams, *J. Mol. Spectrosc.* **1966**, *21*, 76.
[135] O. Dopfer, *Zero kinetic energy (ZEKE) photoelektronenspektroskopie an wasserstoffbrucken-gebundenen phenolkomplexen*, Ph. D. Dissertation, Technische Universitat Munchen, **1994**.
[136] C.-M. Tseng, Y. T. Lee, C.-K. Ni, J.-L. Chang, *J. Phys. Chem. A* **2007**, *111*, 6674.
[137] A. L. Devine, M. G. D. Nix, B. Cronin, M. N. R. Ashfold, *Phys. Chem. Chem. Phys.* **2007**, *9*, 3749.
[138] G. A. King, A. L. Devine, M. G. D. Nix, D. E. Kelly, M. N. R. Ashfold, *Phys. Chem. Chem. Phys.* **2008**, *10*, 6417.
[139] G. A. King, T. A. A. Oliver, R. N. Dixon, M. N. R. Ashfold, *Phys. Chem. Chem. Phys.* **2012**, *14*, 3338.
[140] T. N. V. Karsili, A. M. Wenge, S. J. Harris, D. Murdock, J. N. Harvey, R. N. Dixon, M. N. R. Ashfold, *Chem. Sci.* **2013**, *4*, 2434.
[141] A. G. Sage, T. A. A. Oliver, G. A. King, D. Murdock, J. N. Harvey, M. N. R. Ashfold, *J. Chem. Phys.* **2013**, *138*, 164318.
[142] T. N. V. Karsili, A. M. Wenge, B. Marchetti, M. N. R. Ashfold, *Phys. Chem. Chem. Phys.* **2014**, *16*, 588.
[143] J. D. Young, M. Staniforth, A. S. Chatterley, M. J. Paterson, G. M. Roberts, V. G. Stavros, *Phys. Chem. Chem. Phys.* **2014**, *16*, 550.
[144] S. E. Greenough, M. D. Horbury, J. O. F. Thompson, G. M. Roberts, T. N. V. Karsili, B. Marchetti, D. Townsend, V. G. Stavros, *Phys. Chem. Chem. Phys.* **2014**, *16*, 16187.
[145] M. Staniforth, A. S. Chatterley, J. D. Young, G. M. Roberts, V. G. Stavros, *Biomed. Spectrosc. Imaging* **2014**, *3*, 271.
[146] M. Ataelahi, R. Omidyan, G. Azimi, *Photochem. Photobiol. Sci.* **2015**, *14*, 457.
[147] S. J. Harris, T. N. V. Karsili, D. Murdock, T. A. A. Oliver, A. M. Wenge, D. K. Zaouris, M. N. R. Ashfold, J. N. Harvey, J. D. Few, S. Gowrie, G. Hancock, D. J. Hadden, G. M. Roberts, V. G. Stavros, G. Spighi, L. Poisson, B. Soep, *J. Phys. Chem. A* **2015**, *119*, 6045.
[148] F. Morishima, R. Kusaka, Y. Inokuchi, T. Haino, T. Ebata, *J. Phys. Chem. B* **2015**, *119*, 2557.
[149] F. Morishima, R. Kusaka, Y. Inokuchi, T. Haino, T. Ebata, *Phys. Chem. Chem. Phys.* **2016**, *18*, 8027.
[150] G. A. Cooper, M. R. Cobbin, M. N. R. Ashfold, *J. Phys. Chem. A* **2020**, *124*, 9698.
[151] K. K. Kim, J. Kim, K. C. Woo, S. K. Kim, *J. Phys. Chem. A* **2021**, *125*, 7655.
[152] S. Yamamoto, T. Ebata, M. Ito, *J. Phys. Chem.* **1989**, *93*, 6340.
[153] T. Aota, T. Ebata, M. Ito, *J. Phys. Chem.* **1989**, *93*, 3519.
[154] M. Ito, S. Yamamoto, T. Aota, T. Ebata, *J. Mol. Struct.* **1990**, *237*, 105.
[155] K. Suzuki, Y. Emura, S.-I. Ishiuchi, M. Fujii, *J. Electron Spectrosc. Relat. Phenom.* **2000**, *108*, 13.
[156] J. B. Kim, T. I. Yacovitch, C. Hock, D. M. Neumark, *Phys. Chem. Chem. Phys.* **2011**, *13*, 17378.
[157] C.-W. Cheng, H. Witek, Y.-P. Lee, *J. Chem. Phys.* **2008**, *129*, 154307.
[158] P. Mulder, O. Mozenson, S. Lin, C. E. S. Bernandes, M. E. M. da Piedade, A. F. L. O. M. Santos, M. A. V. R. da Silva, G. A. DiLabio, H.-G. Korth, K. U. Ingold, *J. Phys. Chem. A* **2006**, *110*, 9949.
[159] K. C. Woo, *State- and time-resolved excited-state photodissociation dynamics beyond the Born–Oppenheimer approximation*, Ph. D. Dissertation, Korea Advanced Institute of Science and Technology, Daejeon, Republic of Korea **2019**.
[160] N. Porfido, N. N. Bezuglov, M. Bruvelis, G. Shayeganrad, S. Birindelli, F. Tantussi, I. Guerri, M. Viteau, A. Fioretti, D. Ciampini, M. Allegrini, D. Comparat, E. Arimondo, A. Ekers, F. Fuso, *Phys. Rev. A* **2015**, *92*, 043408.
[161] P. R. Berman, V. S. Malinovsky, *Principles of Laser Spectroscopy and Quantum Optics*, Princeton University Press, Princeton, NJ **2011**.
[162] T. Burgi, S. Leutwyler, *J. Chem. Phys.* **1994**, *101*, 8418.
[163] M. Gerhards, S. Schumm, C. Unterberg, K. Kleinermanns, *Chem. Phys. Lett.* **1998**, *294*, 65.
[164] M. Gerhards, W. Perl, S. Schumm, U. Henrichs, C. Jacoby, K. Kleinermanns, *J. Chem. Phys.* **1996**, *104*, 9362.
[165] D.-S. Ahn, I.-S. Jeon, S.-H. Jang, S.-W. Park, S. Lee, W. Cheong, *Bull. Korean Chem. Soc.* **2003**, *24*, 695.

[166] G. Gregoire, C. Dedonder-Lardeux, C. Jouvet, S. Martrenchard, A. Peremans, D. Solgadi, *J. Phys. Chem. A* **2000**, *104*, 9087.
[167] O. David, C. Dedonder-Lardeux, C. Jouvet, *Int. Rev. Phys. Chem.* **2002**, *21*, 499.
[168] F. J. Hernandez, M. C. Capello, A. Naito, S. Manita, K. Tsukada, M. Miyazaki, M. Fujii, M. Broquier, G. Gregoire, C. Dedonder-Lardeux, C. Jouvet, G. A. Pino, *J. Phys. Chem. A* **2015**, *119*, 12730.
[169] H. S. You, J. Kim, S. Han, D.-S. Ahn, J. S. Lim, S. K. Kim, *J. Phys. Chem. A* **2018**, *122*, 1194.
[170] C. Zhu, H. Nakamura, *J. Chem. Phys.* **1993**, *98*, 6208.
[171] C. Zhu, H. Nakamura, *J. Chem. Phys.* **1994**, *101*, 10630.
[172] C. Zhu, H. Nakamura, *Chem. Phys. Lett.* **1997**, *274*, 205.
[173] C. Zhu, H. Nakamura, *J. Chem. Phys.* **1997**, *107*, 7839.
[174] T. Ishida, S. Nanbu, H. Nakamura, *Int. Rev. Phys. Chem.* **2017**, *36*, 229.

How to cite this article: J. Kim, K. C. Woo, K. K. Kim, M. Kang, S. K. Kim, *Bull. Korean Chem. Soc* **2021**, 1. https://doi.org/10.1002/bkcs.12453